Preprints.org

Technical Note

Not peer-reviewed version

Response of a Triangular Hill Joined with a Semicircular Alluvial Valley under Incident SH Waves

Guangzheng Wang , Jianze Liu * , Zhuang Wang , Yang Li , Xuefeng Zhang , Fazhan Yang

Posted Date: 12 March 2024

doi: 10.20944/preprints202403.0677.v1

Keywords: SH-waves; triangular hill; semicircular alluvial valley; complex function

Preprints.org is a free multidiscipline platform providing preprint service that is dedicated to making early versions of research outputs permanently available and citable. Preprints posted at Preprints.org appear in Web of Science, Crossref, Google Scholar, Scilit, Europe PMC.

Copyright: This is an open access article distributed under the Creative Commons Attribution License which permits unrestricted use, distribution, and reproduction in any medium, provided the original work is properly cited.

Preprints.org (www.preprints.org) | NOT PEER-REVIEWED | Posted: 12 March 2024 doi:10.20944/preprints202403.0677.v1

Disclaimer/Publisher's Note: The statements, opinions, and data contained in all publications are solely those of the individual author(s) and contributor(s) and not of MDPI and/or the editor(s). MDPI and/or the editor(s) disclaim responsibility for any injury to people or property resulting from any ideas, methods, instructions, or products referred to in the content.

Technical Note

Response of a Triangular Hill Joined with a Semicircular Alluvial Valley under Incident SH Waves

Guangzheng Wang, Jianze Liu *, Zhuang Wang, Yang Li, Xuefeng Zhang and Fazhan Yang

Institute of Mechanical and Automotive Engineering, Qingdao University of Technology, Qingdao 266520, China

* Correspondence: liujianze@qut.edu.cn; Tel.: +86-15966766092

Abstract: Under the same seismic load, different local topography will have different effects, which is an important research field in seismic engineering. Hills are connected with valleys is a very typical terrain. Taking this terrain as an example, its response to the most destructive SH waves in the earthquake is studied. By simplifying and dividing the model, the wave functions satisfying the wave equation and boundary conditions in each region are constructed by using the complex function and moving coordinate method. The equations satisfying the boundary continuity conditions are established. With the help of calculation software, the numerical results are obtained. The influence of different parameters on ground motion is discussed.

Keywords: SH-waves; triangular hill; semicircular alluvial valley; complex function

1. Introduction

Earthquake is a very serious natural disaster. It is a worldwide problem to accurately predict earthquakes. To reduce the damage caused by earthquakes, improving the seismic capacity of structures and evaluating the seismic damage is a key point in the field of earthquake engineering. Through previous studies, it is found that under the same seismic load, different local topography will have different effects.

Shear horizontal wave (SH wave) can make the surface shake in the horizontal direction, which is the main cause of earthquake disasters. Many scholars have done a lot of research on the response of different terrains to SH waves. Xu and Han [1] studied the scattering of plane SH waves by multiple semi-cylindrical canyons. Numerical results and discussions of displacements and phases on the surface of the canyons are given. By using the accurate region-matching technique to derive a rigorous series solution, Chang et al. [2] studied the scattering of SH waves by a circular sectorial canyon. Combining the region-matching technique and a periodic indirect boundary element method (PIBEM), Ba and Liang [3] discussed the scattering and diffraction of plane SH waves by periodic alluvial valleys embedded in a layered half-space. Yang et al. [4] investigated the scattering of SH waves around a circular canyon in radial inhomogeneous wedge space. By transforming the governing equation with variable coefficients into a standard Helmholtz equation, the corresponding analytical solution is derived. Qi et al. [5] discussed the scattering of steady-state shear horizontal guided waves from the elastic strip media with multiple semi-cylindrical depressions on the surface and obtained the analytical solution.

The real situation is usually very complex, which is the coupling of many different structures. In this paper, the scattering of SH waves on a hill joined with an alluvial valley is studied. The final solution of the surface response is obtained by using the analytical method.

© 2024 by the author(s). Distributed under a Creative Commons CC BY license.

Preprints.org (www.preprints.org) | NOT PEER-REVIEWED | Posted: 12 March 2024 doi:10.20944/preprints202403.0677.v1

2. Model Simplification and Partition

The hill is simplified as an isosceles triangle, and the alluvial valley is simplified as a semicircle. The simplified model and related parameters are shown in Figure 1. The horizontal surface, the hypotenuse of the triangle, and the boundary of the semicircle are marked as S, C, and S_2, respectively. The mass density of the foundation and sediment is ρ_1 and ρ_2, and the shear modulus is μ_1 and μ_2. SH waves incident in the plane along the X_1-O_1-Y_1 coordinate system at the angle of α.

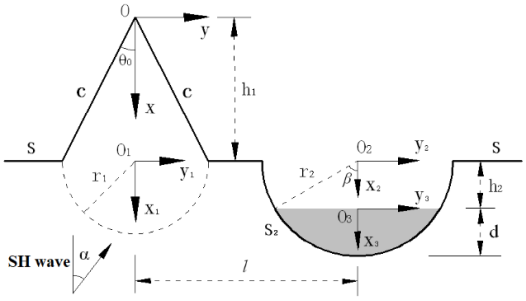

Figure 1. Numerical model of a triangular hill joined with a semi-circular alluvial valley.

The method of "partition and combination" is used to study this complex terrain. As shown in Figure 2, a semicircular virtual boundary S_1 is created with O_1 as the center and r_1 as the radius. Taking S_1 and S_2 as the interface, the model is divided into 3 regions.

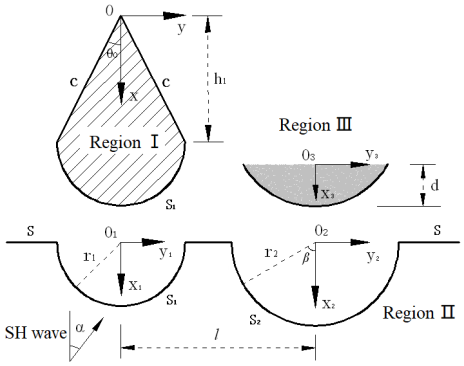

Figure 2. Model of partition.

Wave functions satisfying the boundary conditions are constructed by using the wave function expansion method and coordinate moving method [6–8]. According to the continuous conditions of displacement and stress on the common boundary, the equations are established to solve the unknown coefficients in the wave function of each term. Finally, the dynamic response of each position on the surface can be obtained.

3. Construction of Wave Functions

For steady state, the governing equation of SH waves in isotropic homogeneous and continuous media can be expressed as [9,10]

$$\frac{\partial^2 W}{\partial z \partial \bar{z}} + \frac{1}{4} k^2 W = 0 \tag{1}$$

where W is the displacement function, $k=\omega/C_s$, ω is frequency, $C_s = \sqrt{\mu/\rho}$ is the shear wave velocity.

In polar coordinates, the corresponding stress component is

Preprints.org (www.preprints.org) | NOT PEER-REVIEWED | Posted: 12 March 2024 doi:10.20944/preprints202403.0677.v1

$$\begin{cases} \tau_{rz} = \mu \cdot \dfrac{\partial W}{\partial r} = \mu \cdot \left(\dfrac{\partial W}{\partial z} e^{i\theta} + \dfrac{\partial W}{\partial \bar{z}} e^{-i\theta} \right) \\ \tau_{\theta z} = \dfrac{\mu}{r} \cdot \dfrac{\partial W}{\partial \theta} = i\mu \cdot \left(\dfrac{\partial W}{\partial z} e^{i\theta} - \dfrac{\partial W}{\partial \bar{z}} e^{-i\theta} \right) \end{cases} \tag{2}$$

3.1. Wave Function in Region I

The zero-stress condition on the boundary C is

$$\tau_{\theta z}^{D_1} = \begin{cases} 0, & \theta = +\theta_0 \\ 0, & \theta = -\theta_0 \end{cases} \tag{3}$$

The standing wave function satisfying the governing Equation (1) and boundary condition (3) can be expressed as [11]

$$W^{D_1}(z, \bar{z}) = W_0 \sum_{m=0}^{\infty} A_m J_{mp}(k_1 |z|) \left[\left(\frac{z}{|z|} \right)^{mp} + (-1)^m \left(\frac{z}{|z|} \right)^{-mp} \right] \tag{4}$$

where A_m is the constant to be solved, W_0 is the displacement amplitude. $p=\pi/(2\theta_0)$. $J_{mp}(\cdot)$ is a Bessel function with mp ranks.

The wave function needs to satisfy the continuity condition on S_1 boundary [12,13]. According to the moving coordinate method, Equation (4) in $(z_1, \bar{z}_1)$ the coordinate system can be expressed as

$$W^{D_1}(z_1, \bar{z}_1) = W_0 \sum_{m=0}^{\infty} A_m J_{mp}(k_1 |z_1 + h_1|) \left[\left(\frac{z_1 + h_1}{|z_1 + h_1|} \right)^{mp} + (-1)^m \left(\frac{z_1 + h_1}{|z_1 + h_1|} \right)^{-mp} \right] \tag{5}$$

The corresponding stress can be expressed as

$$\tau_{\eta z_1}^{D_1} = \frac{\mu_1 k_1 W_0}{2} \sum_{m=0}^{\infty} A_m Q_{mp}^1 (z_1 + h_1) \tag{6}$$

where

$$P_t^j(s) = J_{t-1}(k_1|s|) \left(\frac{s}{|s|} \right)^{t-1} e^{i\theta_j} - J_{t+1}(k_1|s|)(-1)^t \left(\frac{s}{|s|} \right)^{-(t+1)} e^{i\theta_j} + J_{t-1}(k_1|s|)(-1)^t \left(\frac{s}{|s|} \right)^{1-t} e^{-i\theta_j} - J_{t+1}(k_1|s|) \left(\frac{s}{|s|} \right)^{t+1} e^{-i\theta_j} \tag{7}$$

3.2. Wave Function in Region III

The boundary condition of the upper surface of sediment can be expressed as

$$\tau_{\theta_3 z_3}^{D_2} = \begin{cases} 0, & \theta_3 = +\dfrac{\pi}{2} \\ 0, & \theta_3 = -\dfrac{\pi}{2} \end{cases} \tag{8}$$

The standing wave function satisfying condition (8) and Equation (1) can be expressed as

$$W^{D_2}(z_3, \bar{z}_3) = W_0 \sum_{m=0}^{\infty} B_m J_m(k_2 |z_3|) \left[\left(\frac{z_3}{|z_3|} \right)^{m} + (-1)^m \left(\frac{z_3}{|z_3|} \right)^{-m} \right] \tag{9}$$

where B_m is the constant to be solved.

According to the moving coordinate method, Equation (9) in $(z_2, \bar{z}_2)$ the coordinate system can be expressed as

Preprints.org (www.preprints.org) | NOT PEER-REVIEWED | Posted: 12 March 2024 doi:10.20944/preprints202403.0677.v1

$$W^{D_2}(z_2,\bar{z}_2)=W_0\sum_{m=0}^{\infty}B_m J_m\left(k_2|z_2-h_2|\right)\left[\left(\frac{z_2-h_2}{|z_2-h_2|}\right)^m+(-1)^m\left(\frac{z_2-h_2}{|z_2-h_2|}\right)^{-m}\right] \tag{10}$$

The corresponding stress can be expressed as

$$\tau_{r_2z_2}^{D_2}=\frac{\mu_2 k_2 W_0}{2}\sum_{m=0}^{\infty}B_m Q_m^2(z_2-h_2) \tag{11}$$

3.3. Scattering Waves in Region II

In region Ⅱ, there are two scattering waves on each boundary because the scattering waves generated by the two depressions interfere with each other. The functions that satisfy the governing equation and the boundary condition can be expressed in the form of multipolar coordinates as [14–16]

$$W^{S_1}(z_j,\bar{z}_j)=W_0\sum_{m=0}^{\infty}C_m H_m^{(1)}\left(k_1|\varepsilon_{1j}|\right)\left[\left(\frac{\varepsilon_{1j}}{|\varepsilon_{1j}|}\right)^m+(-1)^m\left(\frac{\varepsilon_{1j}}{|\varepsilon_{1j}|}\right)^{-m}\right] \tag{12}$$

$$\varepsilon_{1j}=z_1,z_2+id_1;\ j=1,2 \tag{13}$$

$$W^{S_2}(z_j,\bar{z}_j)=W_0\sum_{m=0}^{\infty}D_m H_m^{(1)}\left(k_1|\varepsilon_{2j}|\right)\left[\left(\frac{\varepsilon_{2j}}{|\varepsilon_{2j}|}\right)^m+(-1)^m\left(\frac{\varepsilon_{2j}}{|\varepsilon_{2j}|}\right)^{-m}\right] \tag{14}$$

$$\varepsilon_{2j}=z_1-id_1,z_2;\ j=1,2 \tag{15}$$

The corresponding stress can be expressed as

$$\tau_{r_jz_j}^{S_1}=\frac{\mu_1 k_1 W_0}{2}\sum_{m=0}^{\infty}C_m U_m^j(\varepsilon_{1j}) \tag{16}$$

$$\tau_{r_j\bar{z}_j}^{S_2}=\frac{\mu_1 k_1 W_0}{2}\sum_{m=0}^{\infty}D_m U_m^j(\varepsilon_{2j}) \tag{17}$$

where C_m, D_m are the constant to be solved. $H_m^{(1)}(\cdot)$ is Hankel function of the first kind, and

$$U_t^j(s)=H_{t-1}^{(1)}\left(k_1|s|\right)\left(\frac{s}{|s|}\right)^{t-1}e^{i\theta_j}-H_{t+1}^{(1)}\left(k_1|s|\right)(-1)^t\left(\frac{s}{|s|}\right)^{-(t+1)}e^{i\theta_j}+H_{t-1}^{(1)}\left(k_1|s|\right)(-1)^t\left(\frac{s}{|s|}\right)^{1-t}e^{-i\theta_j}-H_{t+1}^{(1)}\left(k_1|s|\right)\left(\frac{s}{|s|}\right)^{t+1}e^{-i\theta_j} \tag{18}$$

3.4. Incident and Reflected Waves

In the complex plane $(z_j,\bar{z}_j)$, the incident and reflected waves can be expressed as

$$W^{I+R}(z_j,\bar{z}_j)=W_0\sum_{m=0}^{\infty}\frac{\varepsilon_m}{2}(i)^m J_m\left(k_1|\varepsilon_{1j}|\right)\left[(-1)^m e^{im\alpha}+e^{-im\alpha}\right]\left[\left(\frac{\varepsilon_{1j}}{|\varepsilon_{1j}|}\right)^m+(-1)^m\left(\frac{\varepsilon_{1j}}{|\varepsilon_{1j}|}\right)^{-m}\right] \tag{19}$$

The corresponding stress can be expressed as

Preprints.org (www.preprints.org) | NOT PEER-REVIEWED | Posted: 12 March 2024 doi:10.20944/preprints202403.0677.v1

$$\tau_{r_j z_j}^{I+R} = \frac{\mu_1 k_1 W_0}{2} \sum_{m=0}^{\infty} \frac{\varepsilon_m}{2} (i)^m \left[(-1)^m e^{im\alpha} + e^{-im\alpha} \right] P_m^j (\varepsilon_{1j}) \tag{20}$$

where $\varepsilon_0 = 1, \varepsilon_m = 2(m = 1, 2, \cdots)$, and

$$P_t^j(s) = J_{t-1}(k_1|s|)\left(\frac{s}{|s|}\right)^{t-1} e^{i\theta_j} - J_{t+1}(k_1|s|)(-1)^t \left(\frac{s}{|s|}\right)^{-(t+1)} e^{i\theta_j} + J_{t-1}(k_1|s|)(-1)^t \left(\frac{s}{|s|}\right)^{1-t} e^{-i\theta_j} - J_{t+1}(k_1|s|)\left(\frac{s}{|s|}\right)^{t+1} e^{-i\theta_j} \tag{21}$$

4. Establishment of Equations

Wave functions in each region satisfy the continuous conditions of displacement and stress on the common boundary, thus the equations of unknown coefficients can be established as (22). Because there are many parameter variables, the solution is very complex. Due to the space limitation, this article only considers the special case of $d=r_2$.

$$\begin{cases} W^{D_1}(z_1, \bar{z}_1) = W^{S_1}(z_1, \bar{z}_1) + W^{S_2}(z_1, \bar{z}_1) + W^{I+R}(z_1, \bar{z}_1) & z_1 \in S_1 \\ \tau_{\eta z_1}^{D_1} = \tau_{\eta z_1}^{S_1} + \tau_{\eta z_1}^{S_2} + \tau_{\eta z_1}^{I+R} & z_1 \in S_1 \\ W^{D_2}(z_2, \bar{z}_2) = W^{S_1}(z_2, \bar{z}_2) + W^{S_2}(z_2, \bar{z}_2) + W^{I+R}(z_2, \bar{z}_2) & z_2 \in S_2 \\ \tau_{r_2 z_2}^{D_2} = \tau_{r_2 z_2}^{S_1} + \tau_{r_2 z_2}^{S_2} + \tau_{r_2 z_2}^{I+R} & z_2 \in S_2 \end{cases} \tag{22}$$

Expanding (22) by Fourier series in the complex domain, the following equations are obtained

$$\begin{cases} \sum_{n=-\infty}^{+\infty} \sum_{m=0}^{+\infty} X_{nm}^{(1)} A_m - \sum_{n=-\infty}^{+\infty} \sum_{m=0}^{+\infty} Y_{nm}^{(1)} C_m - \sum_{n=-\infty}^{+\infty} \sum_{m=0}^{+\infty} Z_{nm}^{(1)} D_m = \sum_{n=-\infty}^{+\infty} \sum_{m=0}^{+\infty} W_{nm}^{(1)} \\ \sum_{n=-\infty}^{+\infty} \sum_{m=0}^{+\infty} X_{nm}^{(2)} A_m - \sum_{n=-\infty}^{+\infty} \sum_{m=0}^{+\infty} Y_{nm}^{(2)} C_m - \sum_{n=-\infty}^{+\infty} \sum_{m=0}^{+\infty} Z_{nm}^{(2)} D_m = \sum_{n=-\infty}^{+\infty} \sum_{m=0}^{+\infty} W_{nm}^{(2)} \\ \sum_{n=-\infty}^{+\infty} \sum_{m=0}^{+\infty} X_{nm}^{(3)} B_m - \sum_{n=-\infty}^{+\infty} \sum_{m=0}^{+\infty} Y_{nm}^{(3)} C_m - \sum_{n=-\infty}^{+\infty} \sum_{m=0}^{+\infty} Z_{nm}^{(3)} D_m = \sum_{n=-\infty}^{+\infty} \sum_{m=0}^{+\infty} W_{nm}^{(3)} \\ \frac{\mu_2 k_2}{\mu_1 k_1} \sum_{n=-\infty}^{+\infty} \sum_{m=0}^{+\infty} X_{nm}^{(4)} B_m - \sum_{n=-\infty}^{+\infty} \sum_{m=0}^{+\infty} Y_{nm}^{(4)} C_m - \sum_{n=-\infty}^{+\infty} \sum_{m=0}^{+\infty} Z_{nm}^{(4)} D_m = \sum_{n=-\infty}^{+\infty} \sum_{m=0}^{+\infty} W_{nm}^{(4)} \end{cases} \tag{23}$$

The expression of each function is

$$\begin{cases} X_{nm}^{(1)} = \int_{-\frac{\pi}{2}}^{\frac{\pi}{2}} J_{mp}(k_1|z_1 + h_1|) \left[\left(\frac{z_1 + h_1}{|z_1 + h_1|} \right)^{mp} + (-1)^m \left(\frac{z_1 + h_1}{|z_1 + h_1|} \right)^{-mp} \right] e^{-in\theta_1} d\theta_1 \\ Y_{nm}^{(1)} = \int_{-\frac{\pi}{2}}^{\frac{\pi}{2}} H_m^{(1)}(k_1|z_1|) \left[\left(\frac{z_1}{|z_1|} \right)^{m} + (-1)^m \left(\frac{z_1}{|z_1|} \right)^{-m} \right] e^{-in\theta_1} d\theta_1 \\ Z_{nm}^{(1)} = \int_{-\frac{\pi}{2}}^{\frac{\pi}{2}} H_m^{(1)}(k_1|z_1 - id_1|) \left[\left(\frac{z_1 - id_1}{|z_1 - id_1|} \right)^{m} + (-1)^m \left(\frac{z_1 - id_1}{|z_1 - id_1|} \right)^{-m} \right] e^{-in\theta_1} d\theta_1 \\ W_{nm}^{(1)} = \int_{-\frac{\pi}{2}}^{\frac{\pi}{2}} \frac{\varepsilon_m}{2} (i)^m \left[(-1)^m e^{im\alpha} + e^{-im\alpha} \right] J_m(k_1|z_1|) \left[\left(\frac{z_1}{|z_1|} \right)^{m} + (-1)^m \left(\frac{z_1}{|z_1|} \right)^{-m} \right] e^{-in\theta_1} d\theta_1 \end{cases} \tag{24}$$

Preprints.org (www.preprints.org) | NOT PEER-REVIEWED | Posted: 12 March 2024 doi:10.20944/preprints202403.0677.v1

$$\begin{cases} X_{nm}^{(2)} = \int_{-\frac{\pi}{2}}^{\frac{\pi}{2}} Q_{mp}^{1}\left(z_1 + h_1\right) e^{-in\theta_1} d\theta_1 \\ Y_{nm}^{(2)} = \int_{-\frac{\pi}{2}}^{\frac{\pi}{2}} U_m^1\left(z_1\right) e^{-in\theta_1} d\theta_1 \\ Z_{nm}^{(2)} = \int_{-\frac{\pi}{2}}^{\frac{\pi}{2}} U_m^1\left(z_1 - id_1\right) e^{-in\theta_1} d\theta_1 \\ W_{nm}^{(2)} = \int_{-\frac{\pi}{2}}^{\frac{\pi}{2}} \frac{\varepsilon_m}{2} (i)^m \left[(-1)^m e^{im\alpha} + e^{-im\alpha}\right] P_m^1\left(z_1\right) e^{-in\theta_1} d\theta_1 \end{cases} \tag{25}$$

$$\begin{cases} X_{nm}^{(3)} = \int_{-\frac{\pi}{2}}^{\frac{\pi}{2}} J_m\left(k_2 |z_2|\right) \left[\left(\frac{z_2}{|z_2|}\right)^m + (-1)^m \left(\frac{z_2}{|z_2|}\right)^{-m}\right] e^{-in\theta_2} d\theta_2 \\ Y_{nm}^{(3)} = \int_{-\frac{\pi}{2}}^{\frac{\pi}{2}} H_m^{(1)}\left(k_1 |z_2 + id_1|\right) \left[\left(\frac{z_2 + id_1}{|z_2 + id_1|}\right)^m + (-1)^m \left(\frac{z_2 + id_1}{|z_2 + id_1|}\right)^{-m}\right] e^{-in\theta_2} d\theta_2 \\ Z_{nm}^{(3)} = \int_{-\frac{\pi}{2}}^{\frac{\pi}{2}} H_m^{(1)}\left(k_1 |z_2|\right) \left[\left(\frac{z_2}{|z_2|}\right)^m + (-1)^m \left(\frac{z_2}{|z_2|}\right)^{-m}\right] e^{-in\theta_2} d\theta_2 \\ W_{nm}^{(3)} = \int_{-\frac{\pi}{2}}^{\frac{\pi}{2}} \frac{\varepsilon_m}{2} (i)^m \left[\begin{matrix}(-1)^m e^{im\alpha} \\ + e^{-im\alpha}\end{matrix}\right] J_m\left(k_1 |z_2 + id_1|\right) \left[\begin{matrix}(-1)^m \left(\frac{z_2 + id_1}{|z_2 + id_1|}\right)^{-m} \\ + \left(\frac{z_2 + id_1}{|z_2 + id_1|}\right)^m\end{matrix}\right] e^{-in\theta_2} d\theta_2 \end{cases} \tag{26}$$

$$\begin{cases} X_{nm}^{(4)} = \int_{-\frac{\pi}{2}}^{\frac{\pi}{2}} Q_m^2\left(z_2\right) e^{-in\theta_2} d\theta_2 \\ Y_{nm}^{(4)} = \int_{-\frac{\pi}{2}}^{\frac{\pi}{2}} U_m^2\left(z_2 + id_1\right) e^{-in\theta_2} d\theta_2 \\ Z_{nm}^{(4)} = \int_{-\frac{\pi}{2}}^{\frac{\pi}{2}} U_m^2\left(z_2\right) e^{-in\theta_2} d\theta_2 \\ W_{nm}^{(4)} = \int_{-\frac{\pi}{2}}^{\frac{\pi}{2}} \frac{\varepsilon_m}{2} (i)^m \left[(-1)^m e^{im\alpha} + e^{-im\alpha}\right] P_m^2\left(z_2 + id_1\right) e^{-in\theta_2} d\theta_2 \end{cases} \tag{27}$$

(23) are four infinite series equations with unknown coefficients. Finally, the unknown coefficients are obtained by programming.

5. Results Analysis

There is only a standing wave in region Ⅰ and region Ⅲ, so the total wave field is

$$\begin{cases} W_1 = W^{D_1} \\ W_3 = W^{D_2} \end{cases} \tag{28}$$

The total wave field in region Ⅱ consists of three parts:

$$W_2 = W^{S_1} + W^{S_2} + W^{I+R} \tag{29}$$

The incident wave amplitude W_0 is assumed to be 1.0. y_1=0 represents the vertex of the hill, y_1=±r_1 represents the intersection of the hill and the horizontal plane, $|y_1| < r_1$ represents the points on the surface of the hill, y_1/r_1=d_1 represents the center of the alluvial valley. Through numerical examples, the influence of different SH wave numbers (η=2r_1/λ), incident angle, and other parameters on the amplitude of surface displacement is analyzed.

Preprints.org (www.preprints.org) | NOT PEER-REVIEWED | Posted: 12 March 2024 doi:10.20944/preprints202403.0677.v1

When the sediment is softer than the foundation, the variation of surface displacement amplitude with different wave numbers and incident angles is shown in Figure 3. When the wave number is small, the surface displacement changes little, which is similar to the quasi-static problem. With the increase of wave number, the change of surface displacement becomes more and more intense, and the maximum value of displacement amplitude gradually approaches the alluvial valley. When $\eta \geq 0.5$, the surface displacement amplitude in the valley is more than 10, which is 5 times that when the SH wave incident on the horizontal surface.

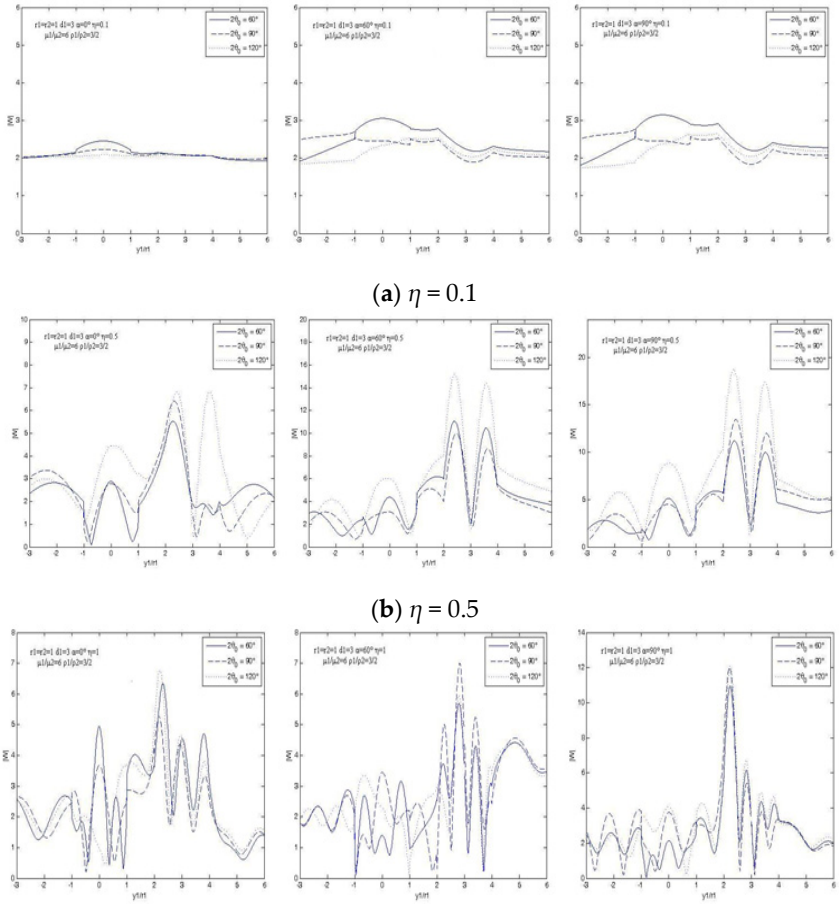

(**a**) $\eta = 0.1$

(**b**) $\eta = 0.5$

(**c**) $\eta = 1$

Figure 3. Surface displacement amplitude (μ_1/μ_2=6, ρ_1/ρ_2=3/2).

When the sediment is harder than the foundation, the surface displacement amplitude with different wave numbers and incident angles is shown in Figure 4, which is much smaller than in Figure 3. The surface displacement in the valley is generally smaller than that of the hill. The maximum value appears at the top of the hill (η=1, α=0°), which is 5.2. When α=0°, the ground motion of the hill increases with the decrease of the vertex angle, and the opposite is true for $\alpha > 0°$.

Preprints.org (www.preprints.org) | NOT PEER-REVIEWED | Posted: 12 March 2024 doi:10.20944/preprints202403.0677.v1

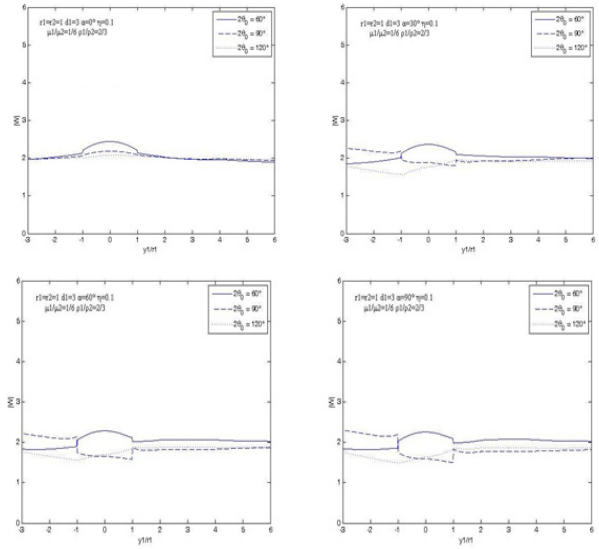

(**a**) $\eta = 0.1$

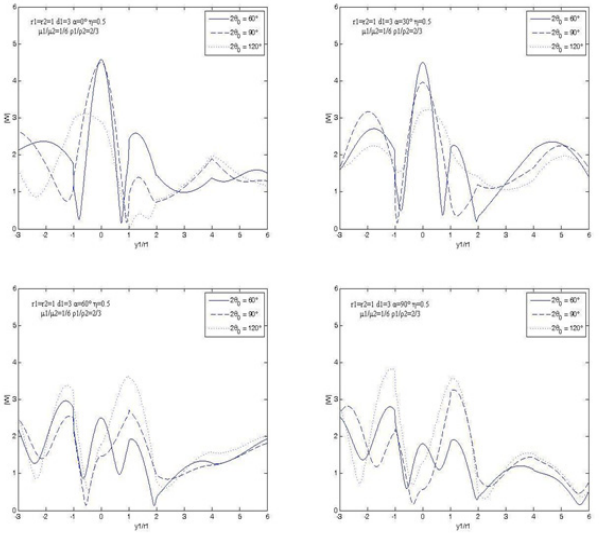

(**b**) $\eta = 0.5$

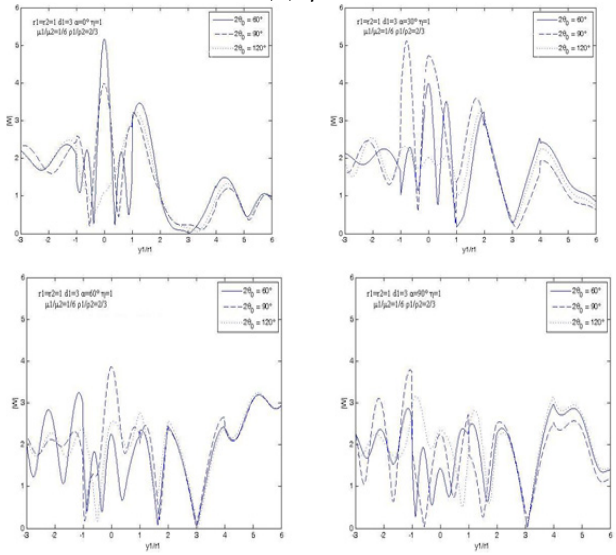

(**c**) $\eta = 1$

Preprints.org (www.preprints.org) | NOT PEER-REVIEWED | Posted: 12 March 2024 doi:10.20944/preprints202403.0677.v1

Figure 4. Surface displacement amplitude (μ_1/μ_2=1/6, ρ_1/ρ_2=2/3).

The average value of surface displacement on the hill is set as e_1. When the SH waves only incident on the hill, the average value of surface displacement is set as e_2. Let $e=e_1/e_2$. Taking the distance between hill and valley as abscissa and e as ordinate, the results are shown in Figure 5. With the increase of distance, e is closer to 1. When $d_1>30r_1$, the difference between e and 1 is less than 0.02. At this time, the interaction between the hill and the valley can be ignored.

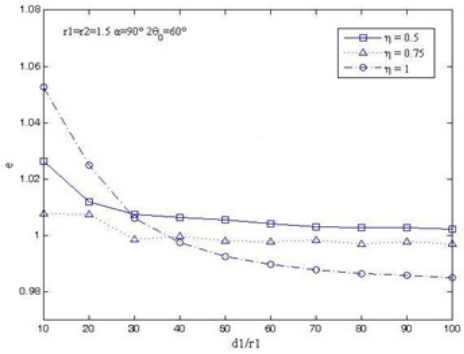

Figure 5. The influence of the alluvial valley on the hill with different distance.

6. Conclusions

Based on elastic wave dynamics and the knowledge of complex functions, the scattering of SH waves on a triangular hill joined with a semicircular alluvial valley is studied. The conclusions are as follows:

1) When the sediment is softer than the foundation, the surface displacement is relatively large as a whole. The maximum value appears near the center of the valley, which is more than 5 times when SH waves incident into the infinite half-space.

2) When the sediment is harder than the foundation, the influence of the valley on the hill is small. The maximum surface displacement appears at the top of the hill, which is more than 2 times when SH waves incident into the infinite half-space.

3) When the distance between the hill and the valley is more than 30 times the half-width of the bottom of the hill, the interaction can be ignored.

Author Contributions: Conceptualization, Jianze Liu and Guangzheng Wang; Funding acquisition, Fazhan Yang and Xuefeng Zhang; Methodology, Jianze Liu, Yang Li and Zhuang Wang; Project administration, Jianze Liu; Software, Jianze Liu and Guangzheng Wang; Visualization, Jianze Liu and Fazhan Yang; Writing – original draft, Jianze Liu and Zhuang Wang; Writing – review & editing, Jianze Liu, Yang Li and Zhuang Wang.

Institutional Review Board Statement: Not applicable.

Informed Consent Statement: Not applicable.

Data Availability Statement: Not applicable.

Conflicts of Interest: The authors declared no potential conflicts of interest concerning the research, authorship, and/or publication of this article.

References

1. Xu Y Y, Han F. Scattering of SH-waves by multiple semi-cylindrical canyons. Earthquake Engineering and Engineering Vibration, 1992, 12(2): 12-18.
2. Chang K H, Tsaur D H, Wang J H. Scattering of SH waves by a circular sectorial canyon. Geophysical Journal International, 2013: 195(1): 532-543.

Preprints.org (www.preprints.org) | NOT PEER-REVIEWED | Posted: 12 March 2024 doi:10.20944/preprints202403.0677.v1

3. Ba Z N, Liang J W. Dynamic response analysis of periodic alluvial valleys under incident plane SH-waves. Journal of Earthquake Engineering, 2016, 21(4): 531-550.
4. Yang Z L, Li X Z, Song Y Q, et al. Scattering of SH waves around circular canyon in inhomogeneous wedge space. Geophysical Journal International, 2020, 223(1): 45-56.
5. Qi H, Yang R J, Guo J, et al. Scattering of SH wave by multiple semi-cylindrical depressions in an elastic strip. Explosion and Shock Waves, 2020, 40(10): 29-41.
6. Shyu W S, Teng T J, Yeh C S. Surface motion of two canyons for incident SH waves by hybrid method. Procedia Engineering, 2014, 79: 533-539.
7. Han F, Liu D K. Research of scattering of plane SH-wave by a semi-cylindrical canyon. Journal of Harbin University of Civil Engineering and Architecture, 1990, 23(3): 24-31.
8. Shashi K, Swapan K C. Influence of scattering of SH-waves in dynamic interaction of shear wall with soil layers. Earthquake Engineering and Engineering Vibration, 2020, 19(3): 583-595.
9. Lv X T, An J B. Ground motion of a semi-cylindrical hill joined with a semi-cylindrical alluvial valley under incident SH-waves. Journal of Vibration and Shock, 2014, 33(17): 127-131+137.
10. Liu Z X, Yu Q, He Y. Effect of randomness of geotechnical medium on the seismic ground motion amplification effect of a sedimentary valley. Acta Seismologica Sinica, 2017, 39(5): 764-777.
11. Chen S H, Zhang Y S. Dynamic responses of canyon with multiple arc-shaped layers under incidence of plane SV waves. Chinese Journal of Geotechnical Engineering, 2017, 39(6): 1074-1081.
12. Gai Z X, Chen C X. Localized boundary element method for seismic wave surface scattering problems: 2D SH case. Chinese Journal of Geophysics, 2020, 63(6): 2274-2280.
13. Xu H N, Zhang Y, Huang Q Y, et al. Ground motion of underground complicated circular lining structure by out-plane wave. Earthquake Engineering and Engineering Dynamics, 2019, 39(6): 154-159.
14. Ma R, Li Y Q, Jing L P, et al. Influence of a semi-circular canyon site on ground surface displacement due to incidence of elastic waves. Earthquake Engineering Journal, 2019, 41(2): 392-398.
15. Liu Q J, Wu Z Y, Vincent W L. Scattering and reflection of SH waves around a slope on an elastic wedged space. Earthquake Engineering and Engineering Vibration, 2019, 18(2): 255-266.
16. Zhou F X, Pang B B, Zhai R Z. Effect of circular tunnels on earthquake subground motions: incidence of SH wave. Earthquake Engineering Journal, 2018, 40(5): 873-878.

Disclaimer/Publisher's Note: The statements, opinions and data contained in all publications are solely those of the individual author(s) and contributor(s) and not of MDPI and/or the editor(s). MDPI and/or the editor(s) disclaim responsibility for any injury to people or property resulting from any ideas, methods, instructions or products referred to in the content.